Monterey Bay Aquarium Research Institute

Characterizing changes in upwelling dynamics under anthropogenic climate change with Spray underwater gliders

Anna Hughes, Carleton College

Mentor: Yui Takeshita

Summer 2020

Keywords: Spray underwater gliders, coastal upwelling, anthropogenic carbon, California Current System

ABSTRACT

The nearshore waters of the California Current System (CCS) have a low aragonite saturation state due to the coastal upwelling of carbon rich waters, making these waters particularly vulnerable to anthropogenic ocean acidification. In order to assess impacts of future ocean acidification, obtaining high spatial and temporal resolution data is vital. Here we show how Spray underwater gliders provide an excellent platform for estimating the anthropogenic carbon signal in the nearshore waters of Monterey Bay and for capturing the high interannual and interseasonal variability of these waters with respect to upwelling. We show how the influx of anthropogenic carbon has led to a shoaling of the saturation horizon, allowing undersaturated waters ($\Omega_{ar} < 1$) to enter the top 100 m of the water column during upwelling season. As anthropogenic ocean acidification progresses, the increased presence of undersaturated waters is projected to have major consequences for the diverse ecosystems that inhabit these waters. Spray underwater gliders provide crucial observations that help to track upwelling and other changing processes, including

deoxygenation and increasing temperature, within the California Current System and other eastern boundary currents with respect to heightened ocean acidification.

INTRODUCTION

Eastern boundary current systems, like the California Current System (CCS), are especially vulnerable to anthropogenic ocean acidification due to the seasonal upwelling of CO_2 rich waters with a low aragonite saturation state (Richard A. Feely et al., 2016; Richard A. Feely et al., 2008; Gruber et al., 2012; C. Hauri et al., 2013). As a result, eastern boundary currents are naturally more acidic and therefore thought to be more vulnerable to anthropogenic ocean acidification (Alin et al., 2012; Claudine Hauri et al., 2009). A common metric for assessing the impact of ocean acidification on ecosystems is saturation state (Ω), particularly the saturation state with respect the aragonite, Ω_{ar} (Richard A. Feely et al., 2012). This term is a measure of the carbonate ion concentration for a given parcel of water, an indication of the thermodynamic potential for aragonite to form or dissolve. An Ω_{ar} of 1 represents the boundary between formation and dissolution of aragonite. Recent hydrographic observations estimate that the saturation horizon ($\Omega_{ar} = 1$) with respect to aragonite has shoaled by approximately 50 to 100 m in the CCS since preindustrial times, bringing undersaturated waters closer to the surface (Alin et al., 2012; Richard A. Feely et al., 2008; R. A. Feely et al., 2002). Progressing ocean acidification, combined with decreasing oxygen concentrations and ocean warming, is expected to have negative consequences for marine coastal ecosystems in the CCS (Bograd et al., 2015; Bograd et al., 2008; Chavez et al., 2017).

Extending from the North Pacific Current (~50˚ N), to Baja California, Mexico (~25˚N), the CCS comprises the eastern limb of the North Pacific Subtropical gyre and is known to experience high variability on both interannual and decadal timescales (Chavez et al., 2017). The CCS is an eastern boundary current and therefore experiences strong coastal upwelling, driven by northwesterly winds in the spring and summer months, that transports cool, nutrient and carbon rich waters closer to the surface. In the CCS, strong coastal upwelling supports many coastal ecosystems and therefore the CCS exhibits high biological productivity, a characteristic common in eastern boundary currents (Messié et al., 2019; Ryther, 1969; Xiu et al., 2018). The nearshore waters of Monterey Bay are situated within the most productive region of the CCS. These waters also, respectively, experience high interannual to interdecadal variability (Bograd et al., 2001; Chavez et al., 2017; C. Hauri et al., 2013). Sustained observations over annual to interannual timescales are needed to make accurate assessments of the impacts of ocean acidification so far and into the future.

Due to the increased productivity of Monterey Bay and the high observed variability, these waters have been repeatedly studied for nearly a century (Chavez et al., 2017). The California Cooperative Oceanic Fisheries Investigations (CalCOFI) have been conducting annual to quarter annual hydrographic cruises along the transect lines, highlighted in yellow in Figure 1, since the 1940s. Studies using these data have identified that the CCS, including the nearshore waters of Monterey Bay, are particularly vulnerable to anthropogenic ocean acidification due to the increased presence of low aragonite saturation state waters during upwelling events (Chavez et al., 2018; Osborne et al., 2020). The increased presence of waters with low aragonite saturation state poses a threat to calcite organisms, in particular pteropods, which are a major food source for important fishery species like salmon (Bednaršek et al., 2018).

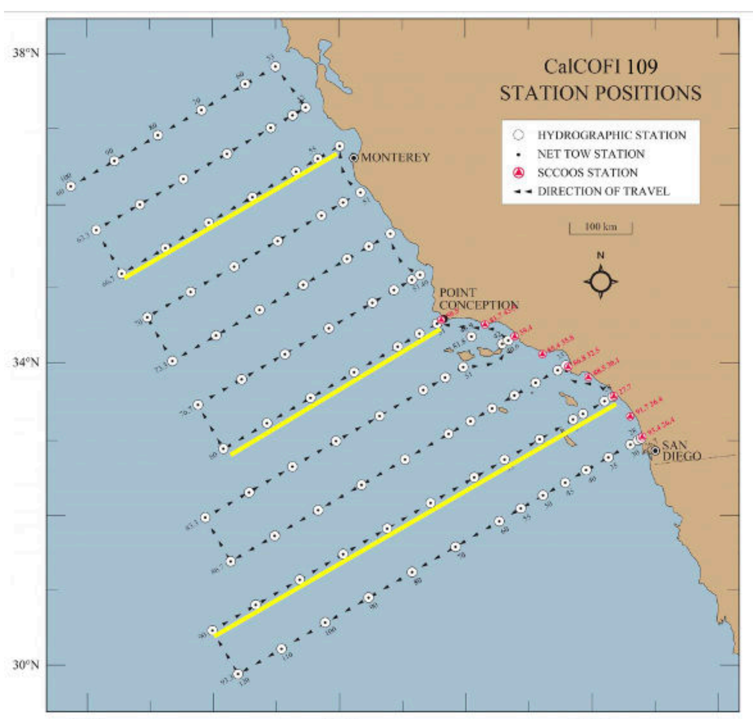

Figure 1. This map shows the CalCOFI transect lines and stations. CalCOFI data was used from line 66.7, stations 50,52.5, and 55. The MBARI gliders also occupied line 66.7 and data from the CUGN was used from line 66.7, limited to the 50 km nearshore. The yellow lines denote the transect lines that are occupied by the CUGN. Photo from CalCOFI station maps (https://www.calcofi.org/graphics/458-station-maps.html).

In order to better understand these rapidly changing dynamics and therefore work to protect these ecosystems, many studies have been conducted using interannual data and modelling approaches to better understand these implications (Gruber et al., 2012; Claudine Hauri et al., 2009; C. Hauri et al., 2013; Takeshita et al., 2015; Xiu et al., 2018). Although these projections are useful in identifying potential future scenarios, they generally lack the high-resolution observations required to capture the interseasonal variability of these waters. This limitation stems from the lack of sustained, high temporal and spatial observations. Due to the time, effort, and money, required to obtain high spatiotemporal resolution data, the current understanding of the variability in the CCS is based mostly on the CalCOFI data from repeat hydrography cruises that occur on quarterly to annual frequencies (Lynn & Simpson, 1987, 1990; Meinvielle & Johnson, 2013). However, it is known that finer scale variability exists in these waters (Nam et al., 2015), additionally, upwelling events in the CCS occur in an episodic manner (C. Hauri et al., 2013), highlighting the need for higher resolution data to better capture the episodic variability of the CCS.

In recent years, the use of autonomous vehicles for higher resolution data collection has increased significantly, specifically, the use of underwater gliders. Spray underwater gliders (Sherman et al., 2001) are autonomous underwater vehicles that move vertically by changing their internal buoyancy and horizontally using wing technology (Rudnick, 2016). These gliders are integrated with a variety of sensors, with the most basic suite measuring temperature, salinity, and pressure, and collect data through conducting profiling dives, in a see-saw pattern, down a max depth of 1000 m. Gliders are useful for sustained observations at relatively good horizontal scales, and because of this, gliders are capable of capturing changes in the CCS on smaller spatiotemporal scales (Rudnick, 2016).

The California Underwater Glider Network (CUGN) has successfully been conducting continuous glider missions along CalCOFI lines 66.7, 80.0, and 90.0, highlighted in yellow in Figure 1, since 2005. The CUGN gliders conduct dives down to 500 m (or bottom depth) and complete these dives in ~3 hours and cover ~ 3 km (Rudnick et al., 2017). Gliders occupy these lines every 2-3 weeks measuring for temperature, salinity, pressure, and velocity. Glider measurements have been evaluated against CalCOFI hydrographic data from these same lines in order to assess glider performance and verify these measurements. The CUGN has shown success in obtaining the high spatiotemporal resolution observations necessary to better understand the episodic variability of the CCS. In addition to providing a foundational understanding of temperature, salinity, and chlorophyll variability, the CUGN has enabled studies of El Niño impacts and provided necessary data for improving high resolution modeling of biogeochemical processes in the CCS (Chao et al., 2018; Jacox et al., 2016; Kurapov et al., 2017; Todd, Rudnick, Davis, et al., 2011; Todd, Rudnick, Mazloff, et al., 2011). For example, Jacox et al. (2016) used glider observations and the Regional Ocean Modeling System to evaluate impacts of the 2015-2016 El Niño event, and demonstrated the capability of these autonomous platforms to assess, in near real time, the regional impacts of the El Niño event. Additionally, Kurapov et al. (2017) were able to evaluate the seasonal and interannual variability of their model using glider observations, due to the high spatiotemporal resolution of the glider data. However, CUGN glider observations are limited due to the basic suite of sensors they contain.

More recently, glider technology has expanded to include the integration of oxygen sensors (Rudnick, 2016); therefore, some of the more recent CUGN glider missions contain oxygen data. Additionally, The Monterey Bay Aquarium Research Institute (MBARI) developed a Deep-Sea DuraFET pH sensor (Johnson et al., 2016) that is able to be integrated into these gliders. Glider missions, conducted in 2019 and 2020 by MBARI, employed gliders suited with this pH sensor. These gliders present a novel way to collect high resolution pH data and provide direct observations of the marine carbonate system, which is critical for understanding and studying ocean acidification. Combining the high spatial and temporal resolution of underwater glider measurements with the technology needed to track anthropogenic climate change enables better understanding of the impacts of anthropogenic ocean acidification in the CCS and the threat posed to these ecosystems.

In this study we work to quantify the anthropogenic carbon signal from MBARI glider observations, in the nearshore waters of Monterey Bay, and apply these estimates to evaluate the effect of increasing anthropogenic carbon on the saturation horizon. This was done using the ΔC* method (Gruber et al., 1996; C. L. Sabine et al., 2002). Using anthropogenic carbon estimates made for glider observations from the MBARI glider missions in 2019 and 2020, we then worked to evaluate the impact of anthropogenic carbon on the interannual upwelling variability by applying these finding to CUGN glider observations.

MATERIALS AND METHODS

GLIDER OBSERVATIONS

Glider missions for May 2019, July 2019, and February 2020, along line 66.7, were conducted by The Monterey Bay Aquarium Research Institute (MBARI), with spray underwater gliders suited with additional sensors: The Deep-Sea DuraFET pH sensor and an oxygen sensor. Glider data from these missions included oxygen, pH, temperature, pressure and salinity measurements. From the data, nutrient concentrations and total alkalinity were estimated from CANYON-B (Bittig et al. 2018). Total dissolved inorganic carbon (DIC), in situ pCO_2, fCO_2, aragonite saturation state, and calcite saturation states were estimated using CO2SYS (Van Heuven et al., 2011) using inputs of total alkalinity (from CANYON-B) and in situ pH (on the total scale) with dissociation constants from Mehrbach et al., 1973 refit by Dickson and Millero, 1987.

HYDROGRAPHIC DATA

The 2016 West Coast Ocean Acidification cruise was conducted from May 5th to June 7th of 2016 aboard the NOAA ship Ronald H. Brown. The cruise took place from Baja California, Mexico to Vancouver Island, Canada and 132 stations were occupied along seventeen transect lines, including CalCOFI line 66.7. For all of the stations, CTD casts were conducted with a rosette-mounted CTD (SBE 9plus, Sea-Bird Scientific), and discrete water samples were collected in Niskin bottles and analyzed. Measured parameters included dissolved oxygen (µmol/kg), DIC (µmol/kg), TA (µmol/kg), pH (on the total scale), and nutrient concentrations (µmol/kg). DIC was measured using coulometric titration (Johnson et al. (1985, 1987)). TA was measured by the potentiometric titration method (Dickson et al., 2003).

The DIC and TA data are both precise and accurate to within 2 µmol/kg. pH was measured on the total scale with the spectrophotometric method described in Byrne et al., 2010 (Feely et al., 2018). The aragonite saturation state values were estimated using CO2SYS (Van Heuven et al., 2011) with inputs of measured total alkalinity and DIC, with dissociation constants from Mehrbach et al., 1973 refit by Dickson and Millero, 1987. Based on DIC and TA measurement uncertainties and the thermodynamic constants the uncertainty in Ω_{ar} is estimated to be ±0.02.

Oxygen analysis was conducted by modified Winkler titration (Carpenter, 1965). Oxygen measurements were estimated to have an uncertainty of ±1 µmol/kg. Nutrient concentrations (phosphate, silicate, and nitrate) were frozen at sea and analyzed later using a Technicon Autoanalyzer II (UNESCO, 1994)at Oregon State University (Feely et al., 2018). Cruise data from May 11th to the 17th of 2019 was collected during the C3PO cruise expedition aboard the R/V Western Flyer. CTD data and bottle data were collected down to 2000 m. The July and May cruises contained 22 and 32 stations respectively. Samples were analyzed aboard the vessel. The cruise reports have not yet been made available, but samples were analyzed similar to those of the 2016 WCOA cruise and measurements were treated with the same uncertainties.

Temperature, salinity, pressure, and oxygen data from annual to biannual CalCOFI cruises from January of 2007 through November of 2019, were obtained for line 66.7 and stations 50.0, 52.5, and 55. These parameters were measured using a Sea-Bird Electronics, Inc., Conductivity-Temperature-Depth (CTD) instrument with a rosette, which was deployed at every station down to a max depth of 515 m, sampling around 20 depths. For all depths, salinity and oxygen were measured and pressures and temperatures were assigned to water samples derived from CTD signals. Salinity and oxygen analyzed as described in the CalCOFI cruise reports for each cruise conducted.

ESTIMATION OF ANTHROPOGENIC CARBON

The method used here to estimate anthropogenic carbon was based on the ΔC^* approach detailed in Sabine et al., 2002, based on the original ΔC^* method introduced by Gruber et al., 1996. The approach assumes that the anthropogenic carbon signal can be isolated from the measured DIC by subtracting off the fraction of DIC associated with biological processes and the preindustrial DIC quantity, with an additional term to account for the disequilibrium of preindustrial waters with the atmosphere. An important assumption made by this method is that the carbon cycle of the ocean has remained in steady state since preindustrial times, therefore assuming that the flux of anthropogenic carbon into the ocean is the only process increasing DIC (Matsumoto and Gruber, 2005). The general approach is shown in equation 1, C_{ant} , C_{meas}, ΔC_{bio}, C_{pre}, and ΔC_{diseq}, denote the anthropogenic carbon signal, the measured DIC quantity, the change in DIC due to biological processes, the preindustrial DIC quantity, and the disequilibrium term, respectively. The calculations of these individual terms are outlined below.

$$C_{ant} = C_{meas} - \Delta C_{bio} - C_{pre} - \Delta C_{diseq} \tag{1}$$

The calculation of the change in DIC due to biological processes was quantified through the same method as Sabine et al. 2002, shown in equation (2) and consists of two parts. The first represents that change in DIC with respect to the remineralization of organic matter while the second part represents the DIC contribution from dissolution of calcium carbonate particles.

$$\Delta C_{bio} = r_{C:O}(AOU) - 0.5(TA_{obs} - TA^{\circ} + r_{N:O}(AOU)) \tag{2}$$

AOU (apparent oxygen utilization) = $O_{2\ sat}$ - $O_{2\ obs}$, where $O_{2\ sat}$ (the saturation oxygen concentration) was calculated using the equations in Garcia and Gordon (1992), and $O_{2\ obs}$ refers to the dissolved oxygen content. TA° represents the performed alkalinity and was estimated using historical TA data in the Pacific (Eq. 3 in Sabine et al. 2002). The r's refer to the remineralization ratios (Anderson and Sarmiento, 1994). The standard error in TA° is ±9 µmol/kg (Sabine et al., 2002). The last term of the ΔC_{bio} calculation accounts for the effect of proton flux on total alkalinity from organic remineralization.

The preindustrial DIC quantity was estimated using CO2SYS (Van Heuven et al., 2011), with TA° and a pCO2 quantity of 280 ppm (the preindustrial atmospheric pCO_2

estimate) as inputs and with dissociation constants from Mehrbach et al., 1973 refit by Dickson and Millero, 1987. Temperature, salinity, pressure, and nutrient data were also used in these estimates, however estimation of C_{pre} differed slightly between ship and glider data, these discrepancies are discussed later.

It has been recognized that the quantifying the ΔC_{diseq} term is one of the most problematic steps in the ΔC^* method. Due to its large associated uncertainty, it is important to make accurate estimates of ΔC_{diseq} (Gruber et al., 1996). An important assumption in evaluating this term is that the global mean air-sea CO_2 disequilibrium has remained constant over time, although this assumption holds for short timescales it breaks down over longer timescales due to the ocean's uptake of anthropogenic carbon (Gruber and Matsumoto, 2005). To account for this, the age of the water mass is generally quantified using tracers such as Chlorofluorocarbons (CFCs) (Sabine and Tanhua, 2010).

In this study, tracer measurements were not made. Instead, ΔC_{diseq} was estimated using previously published values of ΔC_{diseq} for the region with respect to water mass properties (Sabine et al., 2002). The mean θ and salinity were calculated for the potential density (σ_θ) range of the intermediate waters (25.8 k/m^3 < σ_θ < 26.5 k/m^3), and were 9.1 ˚C and 33.9 psu, respectively. This corresponded to a ΔC_{diseq} of -6.24 µmol/kg, water mass (1e) in Sabine et al., 2002.

The denitrification correction, introduced by Sabine et al., 2002, in the biological term, accounts for the denitrification that occurs in the water column. This term uses the N* tracer of Gruber and Sarmiento (1997). The equation for N* is shown in equation 3. This term is then scaled by 106/104 (Deutsch et al., 2001) and subtracted from the ΔC_{bio} term. A sensitivity study of this term was conducted and an uncertainty of ±4 µmol/kg in C_{ant} was estimated to be associated with this term. In low oxygen areas this term becomes more relevant due to increased denitrification, which remineralizes carbon with different stoichiometric ratios to nitrogen than standard aerobic respiration (Sabine et al., 2002). Since the water column had sufficient O_2 (>20 µmol kg^{-1}) where denitrification is unlikely, this term was not included in the presented C_{anth}.

$$N^* = N - 16 * P + 2.9 \qquad (3)$$

The general approach outlined above was adjusted slightly depending on the data set. For gliders, TA_m and DIC_m were determined using empirical algorithms, as explained previously. Comparatively, these quantities were both directly measured for the hydrography data. For gliders, nutrient concentrations were calculated using CANYON-B, whereas cruise data contained measured nutrient concentrations. Therefore, for C_{pre}, the glider estimates used the CANYON-B nutrient estimates. The estimation of TA° required salinity, temperature and phosphate data, therefore the additional uncertainty for TA° in glider anthropogenic carbon estimates is ± 4 μmol/kg. Additionally, for the denitrification term in glider anthropogenic carbon estimates, the uncertainty in estimating both nitrate and phosphate concentrations propagates to an error of ± 5 μmol/kg.

The uncertainty in the anthropogenic carbon estimates associated with random errors can be determined using a first order Taylor series expansion using the respective uncertainties of the measurements required for the calculation (Sabine et al., 1999). For the hydrography anthropogenic carbon estimates, all necessary measurements required to estimate the anthropogenic carbon signal were available, with identified precision values, from cruise reports. These uncertainties propagated to an error of about 10 μmol/kg. For gliders, nutrient, DIC, and TA parameters were calculated using CANYON-B and CO2SYS, therefore an uncertainty of approximately 15 μmol/kg was estimated for glider anthropogenic carbon estimates due to the additional uncertainty introduced in using these empirical algorithms. Additionally, TA° was identified to have standard error of 9 μmol/kg, which was factored into the uncertainty associated with random errors (C. L. Sabine et al., 2002).

There are also potential sources of error associated with the ΔC^* method due to the assumptions made during the calculation, including the estimation of ΔC_{diseq}, calculation of AOU with estimating that O_2 saturation estimates, and the steady state assumptions employed in calculating C_{pre}. Due to these sources of uncertainty, this approach must be used with caution, however, the anthropogenic carbon estimates show good agreement with previously published anthropogenic carbon estimates in the region of study which used the eMLR method to estimate the anthropogenic carbon signal (Feely et al., 2016).

ESTIMATING HISTORICAL Ω_{ar}

Glider data was used also from the California Underwater Glider Network (CUGN). The CUGN observations contain temperature, salinity, and pressure data which are binned in uniform 10 m depth increments. Potential density for CUGN, MBARI glider, and hydrography data was calculated from temperature, salinity, and depth data along line 66.7 from April of 2007 to February of 2020 (Rudnick, 2016), using the SEAWATER library (Morgan, 1994). The glider data from MBARI also contained the aragonite saturation state (Ω_{ar}) parameter calculated using measured pH and TA CANYON-B estimates, the resulting uncertainty associated with Ω_{ar} is ±0.02. A relationship between σ_θ and Ω_{ar} was established using the MBARI glider data using a simple linear regression (Figure 2a). This relationship was used to estimate Ω_{ar} values for the CUGN glider data.

Additionally, a relationship between σ_θ and Ω_{ar} without the influence of anthropogenic carbon was calculated (Figure 2b). Using the MBARI glider data, the anthropogenic carbon estimates were subtracted from the glider DIC estimates. The resulting DIC, without the anthropogenic carbon, was then used with the TA CANYON-B values as inputs to recalculate Ω_{ar} values that do not contain the anthropogenic carbon signal. Using these inputs in CO2SYS, with the original dissociation constants, Ω_{ar} values were recalculated for all the MBARI glider data. A second relationship was then established between σ_θ and the Ω_{ar} values without the influence of anthropogenic carbon using a simple linear regression with potential density. This relationship was then also applied to the CUGN glider data in order to evaluate the impact of anthropogenic carbon across a larger timescale. Additionally, monthly mean Coastal Upwelling Transport Index (CUTI) data, a measure of the vertical transport in the water column, were also used to evaluate the relationships established between Ω_{ar} and σ_θ (Jacox et al., 2018).

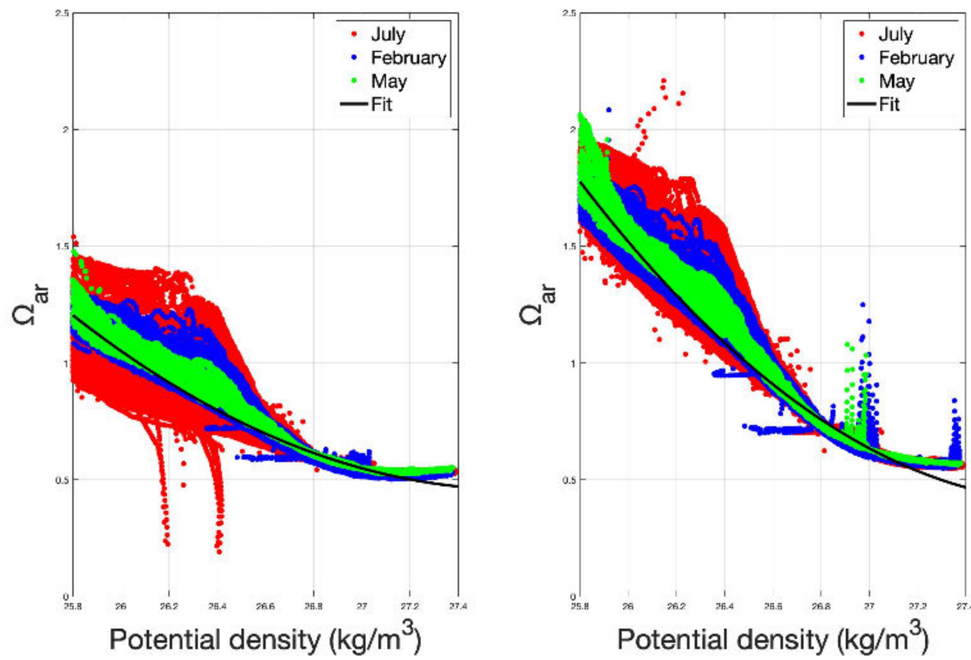

Figure 2. (a) The relationship developed for σ_θ and MBARI glider saturation state values estimated from CO2SYS. (b) The relationship developed for MBARI glider σ_θ and saturation state estimates from CO2SYS after subtracting off the anthropogenic carbon estimates. Red, blue, and green dots show glider observations from July, February, and May respectively. The black lines show the relationship for σ_θ and saturation state identified using a simple linear regression.

RESULTS

GLIDER DATA EVALUATION

The ΔC^* method employs the use of nutrient and TA measurements in its calculation, therefore, the nutrient and TA estimates from CANYON-B, computed for the MBARI gliders, were validated by evaluating the performance of CANYON-B on hydrographic data. Nutrient and TA measurements were available for the May C3PO cruise and were then compared with nutrient and TA estimates, calculated for the May C3PO cruise using CANYON-B. This comparison was done to validate the ability of CANYON-B to accurately estimate these quantities for MBARI glider observations (Figure 3). Figure 3 (a) shows the comparison of TA estimates and measured values showing very strong agreement, especially at high values of TA. Figure 3 (b) and (c) show the comparison for nitrate and phosphate measurements and estimates, respectively. Discrepancies between measured and estimated were not found to be correlated with depth or oxygen. However, both nitrate and phosphate values agreed fairly well, supporting the use of glider nutrient values calculated using CANYON-B.

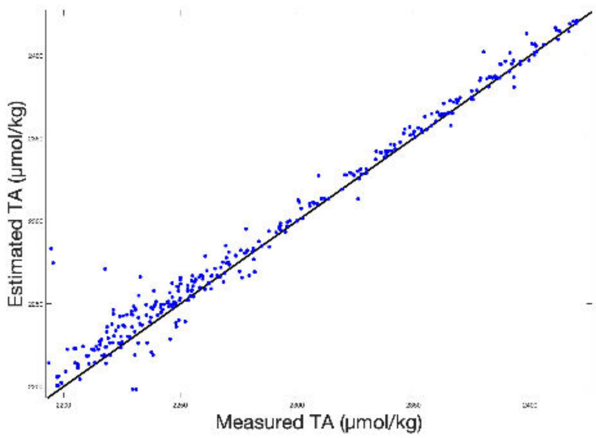

(a)

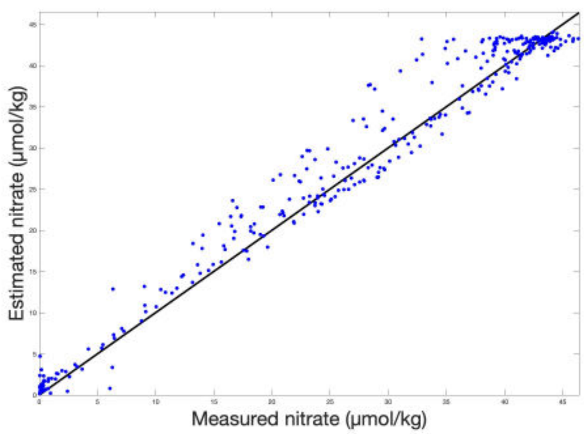

(b)

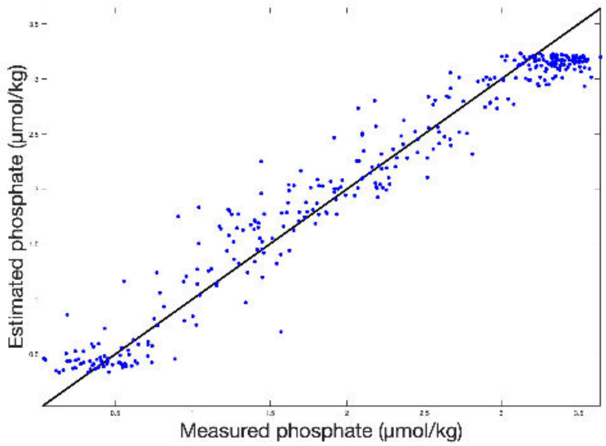

(c)

Figure 3. This figure shows the TA (a), nitrate (b), and phosphate (c) measured and estimated values from the May C3PO hydrographic data. The estimated values were calculated using CANYON-B. The black line in each plot denotes the 1:1 relationship, the value expected if the measured and estimated values were the same.

ANTHROPOGENIC CARBON ESTIMATES

Anthropogenic carbon estimates from the MBARI glider data ranged from 120 to 0 μmol kg^{-1}, generally decreasing with depth as expected (Figure 4). There was significantly higher variability near the surface, where biological production can lead to very high levels of supersaturation of O_2 (up to 130%), which violates the assumption for calculating C_{bio}, where surface O_2 is expected to be in equilibrium with the atmosphere. This is a known shortcoming for the ΔC^* method. However, the C_{anth} estimates were reproducible below a σ_θ of ~26.0. Additionally, good agreement was shown among the MBARI glider observations from May 2019, July 2019, and February 2020. This agreement demonstrates support for the glider anthropogenic carbon estimates, since no significant change in the anthropogenic carbon signal is expected to occur over this time period.

To validate the glider based C_{anth} estimates, we compared these values with anthropogenic carbon estimates from the May C3PO cruise and the 2016 WCOA cruise for the waters below the mixed layer depth, identified for 2019 to be approximately 90 m (Figure 4). The agreement of these estimates demonstrates support of glider measurements. A relationship was developed for the glider anthropogenic carbon estimates for values below a σ_θ of 25.8 kg/m^3 (due to the high variability of surface estimates): y = -41.02x + 1127 (R^2 = 0.96) (Figure 4). The estimates were then compared with published values that were calculated using age tracers (Richard A. Feely et al., 2016). The values agreed well at densities below the mixed layer depth (σ_θ > 26.0 kg/m^3).

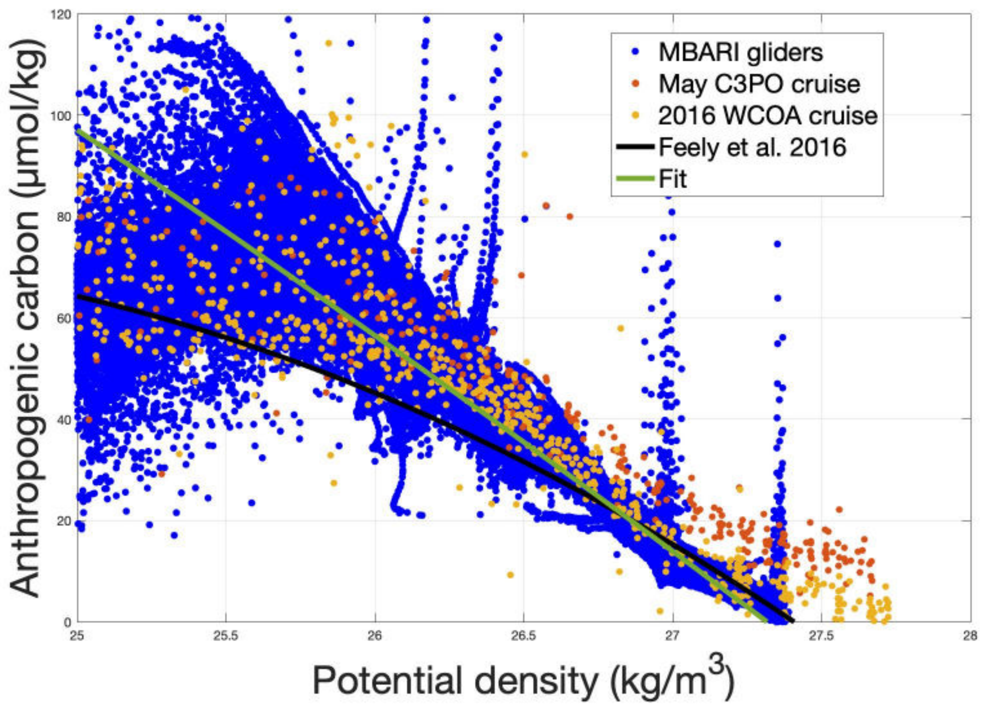

Figure 4. The anthropogenic carbon estimates from the MBARI glider observations (blue dots), 2019 May C3PO cruise (red dots), 2016 WCOA cruise (yellow dots), and the Feely et al., 2016 anthropogenic carbon and σ_θ fit (black line). The fit generated in this study, for σ_θ > 25.8 kg/m^3, is shown in green: y = -41.02x + 1127 (R^2 = 0.96).

CHARACTERIZATION OF INTERANNUAL UPWELLING VARIABILITY

The mean monthly saturation horizon (Ω_{ar} = 1) depths for May, July, and February, were 130 m, 91.9 m, and 157 m, respectively. These depths demonstrate the interseasonal variability of the saturation horizon, specifically, the shoaling of the saturation horizon during upwelling season, with July containing the shallowest mean saturation horizon depth. The saturation states, calculated for the MBARI gliders, average to a mean saturation horizon depth of 126.3 m from May of 2019 to February of 2020. In order to evaluate the interannual variability of upwelling in these waters, the Ω_{ar} data from the MBARI gliders was used to establish a relationship was σ_θ and Ω_{ar} (RMSE = 0.0299). With this relationship, the Ω_{ar} values were estimated for CUGN data from April of 2007 through February of 2020. The percent contributions of waters with Ω_{ar} values of less than 1, between 1 and 1.5, between 1.5 and 2, and greater than 2, in the top 100 m of the water column, for each month that data was available for, were estimated (Figure 5). These estimates show strong seasonal patterns with undersaturated waters increasing in percent contribution during upwelling season, April through October, and decreasing in the winter months (Figure 5).

Additionally, using the relationship established between σ_θ and Ω_{ar} without the influence of anthropogenic carbon (RMSE = 0.0379), the Ω_{ar} values were again estimated for CUGN data from April of 2007 through February of 2020, and the percent contributions of waters with the same ranges of Ω_{ar} were estimated (Figure 6). The same seasonal patterns are observed here, however, even during upwelling season we do not observe the presence of any undersaturated waters ($\Omega_{ar} < 1$) (Figure 6).

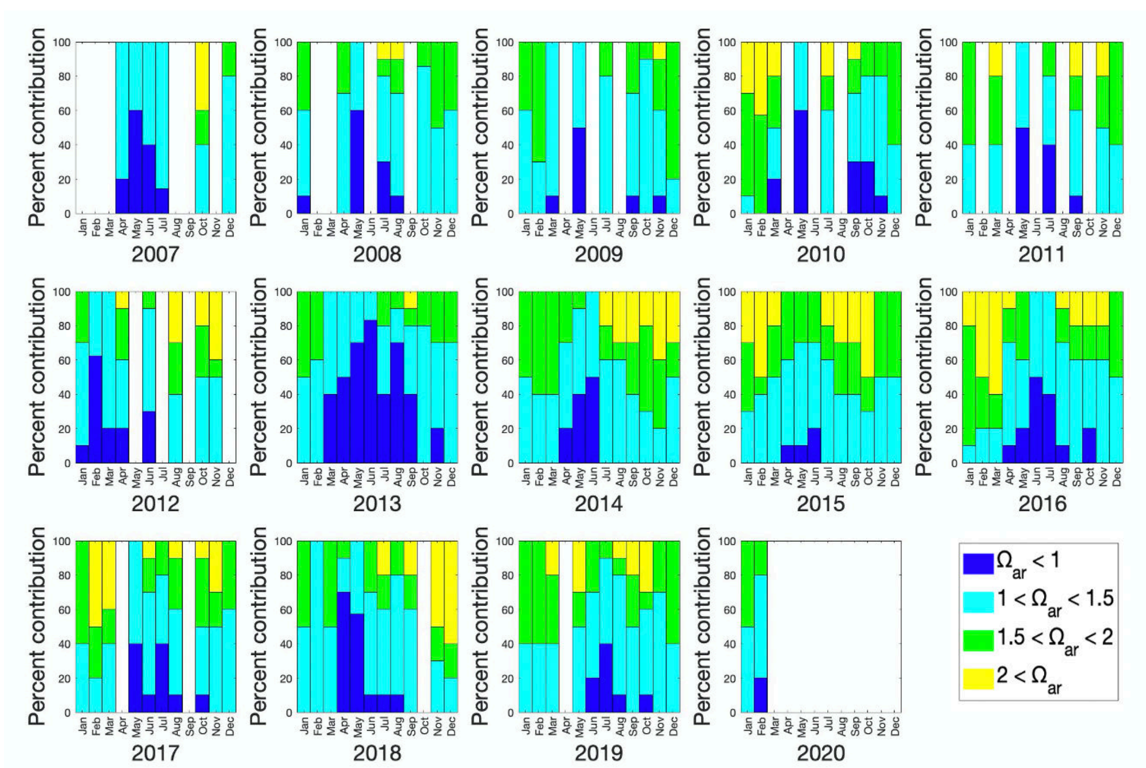

Figure 5. Percent contributions of waters with different Ω_{ar} values for the CUGN glider observations, estimated using σ_θ and Ω_{ar} relationship (Figure 2). Each panel represents the percent contributions of these

waters for a given year (2007-2020), with each bar representing a different month. The gaps are from months without CUGN observations.

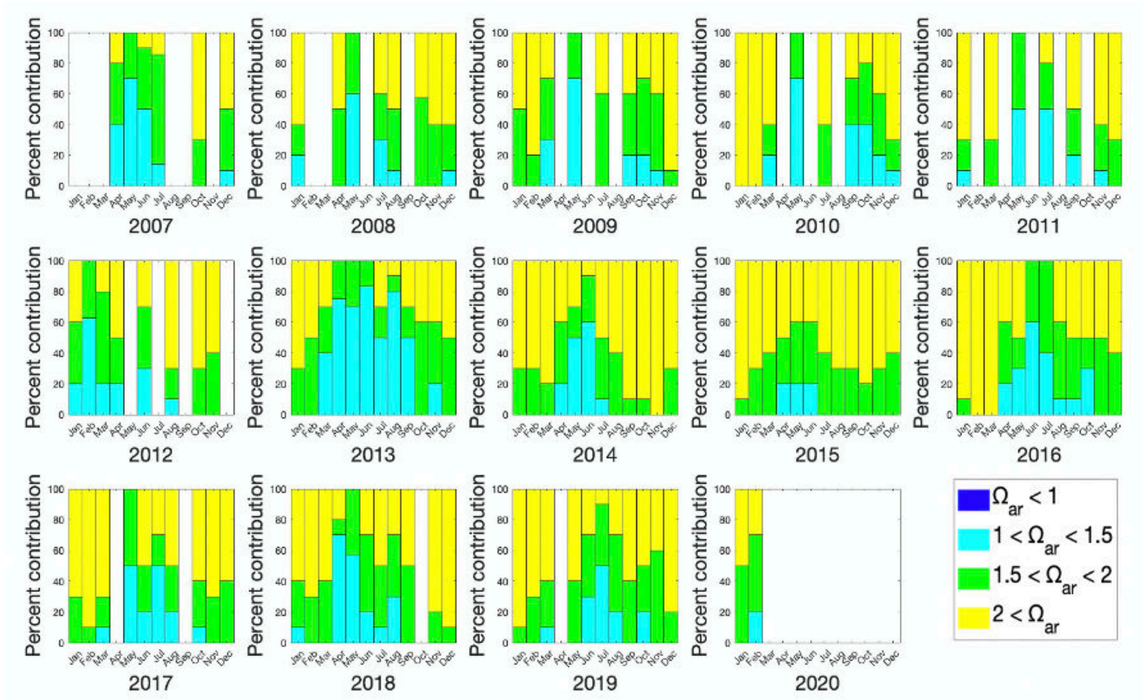

Figure 6. Same as Figure 5, but without anthropogenic carbon

In addition to interseasonal variability, patterns of interannual variability were also observed. Patterns of interannual variability of Ω_{ar} correlated well with the annual cumulative CUTI values. The cumulative CUTI value represents the sum of monthly mean CUTI values, where CUTI is a measure of the vertical transport in the water column. Therefore the annual cumulative CUTI value provides an estimate of total annual vertical transport in the water column. The cumulative CUTI sum correlates well with the percent contribution of corrosive waters in the top 100 m of the water column, weighted by months with available data (Figure 7) ($R^2 = 0.41$). When early years are eliminated, due to gaps in observations, a quadratic relationship is observed ($R^2 = 0.76$). Additionally, when the cumulative CUTI sum is plotted against the mean annual saturation horizon ($\Omega_{ar} = 1$), a strong relationship is also shown (Figure 8) ($R^2 = 0.72$). For this plot, years that lacked observations for four or more months were eliminated.

Using Figure 5 and Figure 6, other trends were also observed, specifically the El Niño events of 2009-2010, 2014-2015, and 2018-2020. These events correlate with decreased upwelling, as shown by (Figure 5, 6). During these years, a lower percent contribution of corrosive waters is observed to be present in the top 100 m of the water column compared with higher percent contribution of corrosive waters during non El Niño years.

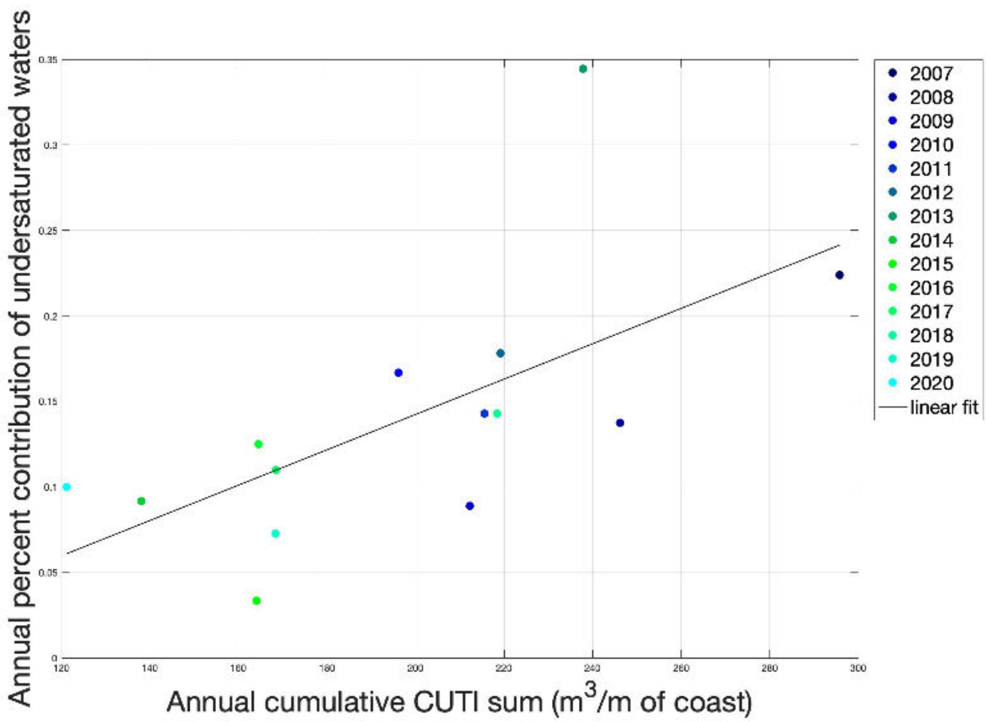

Figure 7. This figure shows the relationship between the annual cumulative CUTI sum and the annual percent contribution of undersaturated waters ($\Omega_{ar} < 1$). The x-axis shows the annual cumulative CUTI sum (m^3/m of coast) and the y-axis shows the annual total percent contribution of undersaturated waters. Each dot represents a different year, detailed in the legend. As shown, these is good correlation between parameters ($R^2 =$ 0.41).

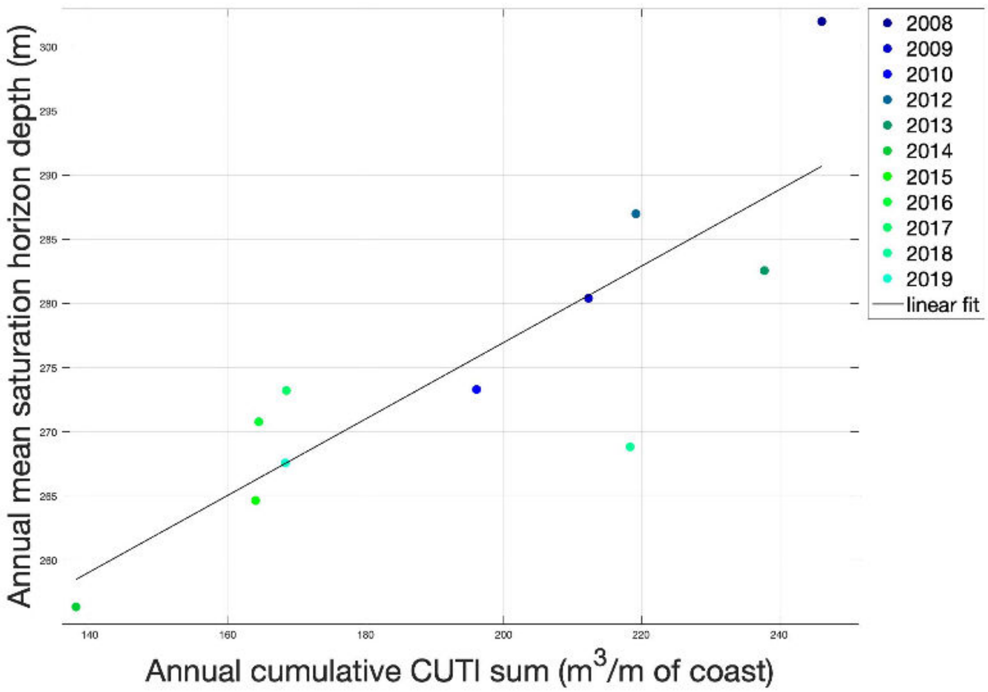

Figure 8. This figure shows the relationship between the annual cumulative CUTI sum and the annual mean saturation horizon depth (Ω_{ar} = 1). The x-axis shows the annual cumulative CUTI sum (m^3/m of coast) and the y-axis shows the annual mean saturation horizon depth (m). Each dot represents a different year, detailed in the legend. Years missing four or months of data were excluded. As shown, these is strong correlation between parameters (R^2 = 0.72).

DISCUSSION

ANTHROPOGENIC CARBON NEAR MONTEREY BAY

The anthropogenic carbon estimates for the MBARI glider, the May C3PO cruise, and the 2016 WCOA cruise agreed within measurement uncertainty. Additionally, when compared with the published values of Feely et al. 2016, the values appear to agree well below the mixed layer depth located at approximately 90 m ($\boldsymbol{\sigma}_\theta$ = 26.0 kg/m^3). Above this depth, both methods break down due to surface water variability (Christopher L. Sabine & Tanhua, 2009). The good agreement of anthropogenic estimates below this depth show support for the use of the ΔC^* method to accurately estimate the anthropogenic carbon signal from glider observations. An important note is that the data used in the Feely et al., 2016 study to create the relationship for σ_θ and anthropogenic carbon (Figure 4) were collected about 10 years prior to the MBARI glider observations (Richard A. Feely et al., 2016). Anthropogenic carbon is estimated to increase on the order of 1 µmol/kg/year (Sarmiento & Gruber, 2002), therefore, this difference could also account for observed discrepancies among the anthropogenic carbon estimates made from the gliders and the Feely et al., 2016 relationship.

The ΔC* method has received critique for its ability to accurately estimate the anthropogenic carbon signal (Matsumoto & Gruber, 2005; Christopher L. Sabine & Tanhua, 2009). The method used by Feely et al., 2016 to estimate the anthropogenic carbon estimates that created the σ_θ vs. anthropogenic carbon relationship (Figure 4) used the eMLR method, an approach that compensates for temporal and water mass distribution variability and is considered a more sophisticated way to estimate this quantity (Christopher L. Sabine & Tanhua, 2009). However, the good agreement between the Feely et al. estimates and the estimates made here using the ΔC* method provide good support of the ability of the ΔC* method to estimate the anthropogenic carbon signal.

The sensitivity of the CCS in the face of increasing anthropogenic ocean acidification is a direct result of the role that upwelling plays in transporting the carbon rich waters of the ocean interior closer to the surface in coastal waters (Chan et al., 2017; Gruber et al., 2012). Therefore, accurately estimating the anthropogenic carbon quantity is critical in understanding the change in this value over time, and thus the impact that increasing anthropogenic carbon is projected to have on upwelling. We have demonstrated that glider observations with pH sensors can potentially provide these measurements, thus, could provide a powerful tool to further our understanding of the impacts of ocean acidification in the CCS.

UPWELLING REPERCUSSIONS IN THE CCS

The Ω_{ar} values calculated for the MBARI gliders showed a mean saturation horizon depth of 126.3 m for the data collected from May 2019 through February of 2020. Hauri et al. (2009, 2013) and Gruber et al. (2012) note the observed shoaling of the saturation horizon by about 150 m since preindustrial times and projected continued shoaling by an additional 100 to 150 m by 2050, with undersaturated waters breaking the surface during upwelling season. As shown in Figures 4,5, and 6, upwelling in the CCS exhibits high interannual variability and strong seasonal patterns where waters with lower aragonite saturation states increase in percent contribution within the top 100 m of the water column, during upwelling season. Hauri et al. (2009) and Gruber et al. (2012), both employed the use of eddy-resolving models to capture this trend and extended their models till 2050, to evaluate how upwelling is projected to be affected by anthropogenic ocean acidification and what the repercussions are for marine coastal ecosystems. Here, upwelling variability was only explored from 2007 through 2020, but used glider observations. Both Hauri et al. (2009) and Gruber et al. (2012) showed similar seasonal variation, with increasing presence of undersaturated waters with respect to aragonite, increasing in percent contribution, between 2007 and 2020, as shown in this study. Both studies note the expected increase in presence of undersaturated waters during upwelling season in future years as well as a continued shoaling of the saturation horizon by an additional 75 m to 100 m by 2050.

Both Hauri et al. and Gruber et al., in addition to other studies, highlight that pH and saturation state are projected to decrease as a result of increasing anthropogenic carbon uptake. Gruber et al. (2012) and Hauri et al. (2013) also both note a projected shoaling of the saturation horizon by an additional 75 m to 100 m by 2050, possibly moving it into the upper 100 m year-round (Claudine Hauri et al., 2009). As shown in Figure 8, the mean annual depth of the saturation horizon has a strong correlation with the cumulative CUTI sum (an estimate of the annual total vertical transport). Additionally, as shown in Figure 7 the cumulative CUTI sum has also correlated with total percent contribution of undersaturated waters in the upper 100 m. These relationships demonstrate that as anthropogenic carbon increases, leading to a shoaling of the saturation horizon. This implication is also shown in the progressively shallower annual mean saturation horizon depth from 2008 to 2019 (Figure 8). Following these trends, an increased uptake in anthropogenic carbon therefore leads to an increase in the presence of undersaturated waters in the top 100 m, aligning with the findings in Hauri et al. and Gruber et al.

The percent contributions were estimated using the σ_θ and Ω_{ar} relationship developed from the MBARI glider missions in 2019 and 2020. Therefore, these percent contributions are estimations. These estimates are supported by seasonal trends demonstrated in Hauri et al. (2009) and Gruber et al. (2012) and expected trends of El Niño events and upwelling. Additionally, not all months from 2007 through 2020 had CUGN data, therefore, as shown in Figures 4 and 5, some months are missing data, which could lead to discrepancies in percent contribution estimates annual percent contribution ratio, shown in Figure 7. Continued glider missions are important in providing consistent observations in order to evaluate seasonal processes, like upwelling.

ROLE OF GLIDERS IN ADVANCING OCEAN RESEARCH

Accurately estimating the anthropogenic signal is important for developing an understanding of the role anthropogenic carbon plays in ocean process like ocean acidification and the shoaling of the saturation horizon (Caldeira & Wickett, 2003; Richard A. Feely et al., 2016; Gruber et al., 2012; C. Hauri et al., 2013; Khatiwala et al., 2013). The NOAA Acidification Research Plan 2020-2029 notes one of the main research objectives of the next decade in the West Coast region is to “improve characterization of OA parameters in subsurface environments that are critical habitats to commercially and ecologically important species” (Busch et al., 2020). Some actions they note, required to achieve this goal, are to enhance profiling platforms “to include additional chemical and biological sensors for subsurface waters to delineate rates of change of critical parameters” and “continue to quantify anthropogenic CO_2 concentrations through coastal and open ocean cruises, which collect the data needed to attribute carbonate chemistry change to anthropogenic acidification versus contributions from other processes” (Busch et al., 2020).

As shown here, gliders were able to accurately estimate the anthropogenic carbon signal within the measurement uncertainty of cruise data. The coupled impacts of ocean acidification, deoxygenation, and increased temperature pose a great threat to marine ecosystems. As demonstrated, gliders, suited with pH and oxygen sensors, are able to measure for pH, oxygen, and temperature, providing necessary information in order to improve characterization of ocean acidification parameters in subsurface environments. Gliders show incredible potential in helping to achieve the research objectives highlighted for the next decade.

CONCLUSION

Here we worked to show how Spray underwater gliders provide a useful mechanism for providing high spatial and temporal, autonomous observations of coastal ocean dynamics. When integrated with pH sensors, these gliders are able to accurately estimate the anthropogenic carbon quantity within measurement uncertainty, in addition to providing high quality, interseasonal and interannual observations of upwelling variability. The high spatial and temporal resolution data obtained by these gliders have been shown to capture changes related to interannual upwelling variation, El Niño events and marine heat waves experienced by the nearshore waters of Monterey Bay. These results demonstrate how underwater gliders provide a useful platform for better understanding anthropogenic carbon effects on the highly variable waters of the California Current System, an area especially vulnerable to anthropogenic ocean acidification. Additionally, this study shows the potential application of glider use in evaluating other eastern boundary current systems in order to better understand what these changes could mean for coastal ecosystems.

ACKNOWLEDGEMENTS

I would first like to thank my mentor, Yui Takeshita, for providing the opportunity for me to further my exploration of the field of biogeochemical oceanography, and for his guidance throughout the completion of my project. I would also like to thank my co-intern Brooke Hale for her helpful advice throughout the internship. Additionally, I want to thank George Matsumoto, Megan Bassett, Tatjana Ellis, and my fellow interns for their support over the course of this summer. I am especially grateful for their resilience in the face of a novel virtual internship. I am also grateful to the MBARI staff for their effort in accommodating changes resulting from this being a virtual internship. I would like to end by thanking the Kolenkow-Reitz fellowship for funding this opportunity.

REFERENCES

Alin, S. R., Feely, R. A., Dickson, A. G., Hernández-Ayón, J. M., Juranek, L. W., Ohman, M. D., & Goericke, R. (2012). Robust empirical relationships for estimating the carbonate system in the southern California Current System and application to CalCOFI hydrographic cruise data (2005–2011). *Journal of Geophysical Research: Oceans, 117*(C5). https://doi.org/10.1029/2011JC007511

Bednaršek, N., Feely, R. A., Beck, M. W., Glippa, O., Kanerva, M., & Engström-Öst, J. (2018). El Niño-Related Thermal Stress Coupled With Upwelling-Related Ocean Acidification Negatively Impacts Cellular to Population-Level Responses in Pteropods Along the California Current System With Implications for Increased Bioenergetic Costs. *Frontiers in Marine Science, 5*, 486. 10.3389/fmars.2018.00486. https://www.frontiersin.org/article/10.3389/fmars.2018.00486

Bograd, S. J., Buil, M. P., Lorenzo, E. D., Castro, C. G., Schroeder, I. D., Goericke, R., et al. (2015). Changes in source waters to the Southern California Bight. *Deep Sea Research Part II: Topical Studies in Oceanography, 112*, 42-52. http://www.sciencedirect.com/science/article/pii/S096706451400126X

Bograd, S. J., Castro, C. G., Di Lorenzo, E., Palacios, D. M., Bailey, H., Gilly, W., & Chavez, F. P. (2008). Oxygen declines and the shoaling of the hypoxic boundary in the California Current. *Geophysical Research Letters, 35*(12). https://doi.org/10.1029/2008GL034185

Bograd, S. J., Chereskin, T. K., & Roemmich, D. (2001). Transport of mass, heat, salt, and nutrients in the southern California Current System: Annual cycle and interannual variability. *Journal of Geophysical Research: Oceans, 106*(C5), 9255-9275. https://doi.org/10.1029/1999JC000165

Caldeira, K., & Wickett, M. E. (2003). Anthropogenic carbon and ocean pH. *Nature, 425*(6956), 365-365. https://doi.org/10.1038/425365a

Chan, F., Barth, J. A., Blanchette, C. A., Byrne, R. H., Chavez, F., Cheriton, O., et al. (2017). Persistent spatial structuring of coastal ocean acidification in the California Current System. *Scientific Reports, 7*(1), 2526. https://doi.org/10.1038/s41598-017-02777-y

Chao, Y., Farrara, J. D., Zhang, H., Armenta, K. J., Centurioni, L., Chavez, F., et al. (2018). Development, implementation, and validation of a California coastal ocean modeling, data assimilation, and forecasting system. *Deep Sea Research Part II: Topical Studies in Oceanography, 151*, 49-63. http://www.sciencedirect.com/science/article/pii/S096706451630025X

Chavez, F. P., Pennington, J. T., Michisaki, R. P., Blum, M., Chavez, G. M., Friederich, J., et al. (2017). Climate Variability and Change Response of a Coastal Ocean Ecosystem. *Oceanography, 30*(4), 128-145. www.jstor.org/stable/26367631

Chavez, F. P., Sevadjian, J., Wahl, C., Friederich, J., & Friederich, G. E. (2018). Measurements of pCO2 and pH from an autonomous surface vehicle in a coastal upwelling system. *Deep Sea Research Part II: Topical Studies in Oceanography, 151*, 137-146. http://www.sciencedirect.com/science/article/pii/S0967064516302338

Feely, R. A., Alin, S. R., Carter, B., Bednaršek, N., Hales, B., Chan, F., et al. (2016). Chemical and biological impacts of ocean acidification along the west coast of

North America. *Estuarine, Coastal and Shelf Science, 183*, 260-270. http://www.sciencedirect.com/science/article/pii/S0272771416302980

Feely, R. A., Sabine, C. L., Byrne, R. H., Millero, F. J., Dickson, A. G., Wanninkhof, R., et al. (2012). Decadal changes in the aragonite and calcite saturation state of the Pacific Ocean. *Global Biogeochemical Cycles, 26*(3). https://doi.org/10.1029/2011GB004157

Feely, R. A., Sabine, C. L., Hernandez-Ayon, J. M., Ianson, D., & Hales, B. (2008). Evidence for Upwelling of Corrosive "Acidified" Water onto the Continental Shelf. *Science, 320*(5882), 1490. http://science.sciencemag.org/content/320/5882/1490.abstract

Feely, R. A., Sabine, C. L., Lee, K., Millero, F. J., Lamb, M. F., Greeley, D., et al. (2002). In situ calcium carbonate dissolution in the Pacific Ocean. *Global Biogeochemical Cycles, 16*(4), 91-91-91-12. https://doi.org/10.1029/2002GB001866

Gruber, N., Hauri, C., Lachkar, Z., Loher, D., Frölicher, T. L., & Plattner, G.-K. (2012). Rapid Progression of Ocean Acidification in the California Current System. *Science, 337*(6091), 220. http://science.sciencemag.org/content/337/6091/220.abstract

Gruber, N., Sarmiento, J. L., & Stocker, T. F. (1996). An improved method for detecting anthropogenic CO2 in the oceans. *Global Biogeochemical Cycles, 10*(4), 809-837. https://agupubs.onlinelibrary.wiley.com/doi/abs/10.1029/96GB01608

Hauri, C., Gruber, N., Plattner, G.-K., Alin, S., Feely, R. A., Hales, B., & Wheeler, P. A. (2009). OCEAN ACIDIFICATION IN THE CALIFORNIA CURRENT SYSTEM. *Oceanography, 22*(4), 60-71. www.jstor.org/stable/24861024

Hauri, C., Gruber, N., Vogt, M., Doney, S. C., Feely, R. A., Lachkar, Z., et al. (2013). Spatiotemporal variability and long-term trends of ocean acidification in the California Current System. *Biogeosciences, 10*(1), 193-216. https://bg.copernicus.org/articles/10/193/2013/

Jacox, M. G., Edwards, C. A., Hazen, E. L., & Bograd, S. J. (2018). Coastal Upwelling Revisited: Ekman, Bakun, and Improved Upwelling Indices for the U.S. West Coast. *Journal of Geophysical Research: Oceans, 123*(10), 7332-7350. https://doi.org/10.1029/2018JC014187

Jacox, M. G., Hazen, E. L., Zaba, K. D., Rudnick, D. L., Edwards, C. A., Moore, A. M., & Bograd, S. J. (2016). Impacts of the 2015–2016 El Niño on the California Current System: Early assessment and comparison to past events. *Geophysical Research Letters, 43*(13), 7072-7080. https://doi.org/10.1002/2016GL069716

Johnson, K. S., Jannasch, H. W., Coletti, L. J., Elrod, V. A., Martz, T. R., Takeshita, Y., et al. (2016). Deep-Sea DuraFET: A Pressure Tolerant pH Sensor Designed for Global Sensor Networks. *Analytical Chemistry, 88*(6), 3249-3256. https://doi.org/10.1021/acs.analchem.5b04653

Khatiwala, S., Tanhua, T., Fletcher, S. M., Gerber, M., Doney, S. C., Graven, H. D., et al. (2013). Global ocean storage of anthropogenic carbon. *Biogeosciences, 10*(4), 2169-2191. <Go to ISI>://WOS:000318434200001

Kurapov, A. L., Pelland, N. A., & Rudnick, D. L. (2017). Seasonal and interannual variability in along-slope oceanic properties off the US West Coast: Inferences from a high-resolution regional model. *Journal of Geophysical Research: Oceans, 122*(7), 5237-5259. https://doi.org/10.1002/2017JC012721

Lynn, R. J., & Simpson, J. J. (1987). The California Current system: The seasonal variability of its physical characteristics. *Journal of Geophysical Research: Oceans, 92*(C12), 12947-12966. https://doi.org/10.1029/JC092iC12p12947

Lynn, R. J., & Simpson, J. J. (1990). The flow of the undercurrent over the continental borderland off southern California. *Journal of Geophysical Research: Oceans, 95*(C8), 12995-13008. https://doi.org/10.1029/JC095iC08p12995

Matsumoto, K., & Gruber, N. (2005). How accurate is the estimation of anthropogenic carbon in the ocean? An evaluation of the ΔC* method. *Global Biogeochemical Cycles, 19*(3). https://doi.org/10.1029/2004GB002397

Meinvielle, M., & Johnson, G. C. (2013). Decadal water-property trends in the California Undercurrent, with implications for ocean acidification. *Journal of Geophysical Research: Oceans, 118*(12), 6687-6703. https://doi.org/10.1002/2013JC009299

Messié, M., Northcott, D., Fiechter, J., Santora, J., & Chavez, F. (2019). *Biological production and zooplankton hotspots in Eastern Boundary Upwelling Systems*. https://ui.adsabs.harvard.edu/abs/2019EGUGA..2116229M

Morgan, P. P. (1994). *SEAWATER : a library of MATLAB computational routines for the properties of sea water / Phillip P. Morgan*. Hobart, Tas: CSIRO Marine Laboratories.

Nam, S., Takeshita, Y., Frieder, C. A., Martz, T., & Ballard, J. (2015). Seasonal advection of Pacific Equatorial Water alters oxygen and pH in the Southern California Bight. *Journal of Geophysical Research: Oceans, 120*(8), 5387-5399. https://doi.org/10.1002/2015JC010859

Osborne, E. B., Thunell, R. C., Gruber, N., Feely, R. A., & Benitez-Nelson, C. R. (2020). Decadal variability in twentieth-century ocean acidification in the California Current Ecosystem. *Nature Geoscience, 13*(1), 43-49. https://doi.org/10.1038/s41561-019-0499-z

Rudnick, D. L. (2016). Ocean Research Enabled by Underwater Gliders. *Annual Review of Marine Science, 8*(1), 519-541. https://www.annualreviews.org/doi/abs/10.1146/annurev-marine-122414-033913

Rudnick, D. L., Zaba, K. D., Todd, R. E., & Davis, R. E. (2017). A climatology of the California Current System from a network of underwater gliders. *Progress in Oceanography, 154*, 64-106. http://www.sciencedirect.com/science/article/pii/S0079661116302075

Ryther, J. H. (1969). Photosynthesis and Fish Production in the Sea. *Science, 166*(3901), 72. http://science.sciencemag.org/content/166/3901/72.abstract

Sabine, C. L., & Tanhua, T. (2009). Estimation of Anthropogenic CO2 Inventories in the Ocean. *Annual Review of Marine Science, 2*(1), 175-198. https://doi.org/10.1146/annurev-marine-120308-080947

Sabine, C. L., Feely, R. A., Key, R. M., Bullister, J. L., Millero, F. J., Lee, K., et al. (2002). Distribution of anthropogenic CO2 in the Pacific Ocean. *Global Biogeochemical Cycles, 16*(4), 30-31-30-17. https://agupubs.onlinelibrary.wiley.com/doi/abs/10.1029/2001GB001639

Sarmiento, J. L., & Gruber, N. (2002). Sinks for Anthropogenic Carbon. *Physics Today, 55*(8), 30-36. https://doi.org/10.1063/1.1510279

Sherman, J., Davis, R. E., Owens, W. B., & Valdes, J. (2001). The autonomous underwater glider "Spray". *IEEE Journal of Oceanic Engineering, 26*(4), 437-446.

Takeshita, Y., Frieder, C. A., Martz, T. R., Ballard, J. R., Feely, R. A., Kram, S., et al. (2015). Including high-frequency variability in coastal ocean acidification projections. *Biogeosciences, 12(19), 5853-5870.* Journal Article. https://repository.library.noaa.gov/view/noaa/16507

Todd, R. E., Rudnick, D. L., Davis, R. E., & Ohman, M. D. (2011). Underwater gliders reveal rapid arrival of El Niño effects off California's coast. *Geophysical Research Letters, 38*(3). https://doi.org/10.1029/2010GL046376

Todd, R. E., Rudnick, D. L., Mazloff, M. R., Davis, R. E., & Cornuelle, B. D. (2011). Poleward flows in the southern California Current System: Glider observations and numerical simulation. *Journal of Geophysical Research: Oceans, 116*(C2). https://doi.org/10.1029/2010JC006536

Xiu, P., Chai, F., Curchitser, E. N., & Castruccio, F. S. (2018). Future changes in coastal upwelling ecosystems with global warming: The case of the California Current System. *Scientific Reports, 8*(1), 2866. https://doi.org/10.1038/s41598-018-21247-7